Hindawi
Advances in Civil Engineering
Volume 2019, Article ID 4950841, 11 pages
https://doi.org/10.1155/2019/4950841

Research Article

Vibration Theoretical Analysis of Elastically Connected Multiple Beam System under the Moving Oscillator

Binbin He[1,2] **and Yulin Feng**[3,4]

[1]*State Key Laboratory of Frozen Soil Engineering, Northwest Institute of Eco-Environment and Resources, Chinese Academy of Sciences, Lanzhou 730000, China*
[2]*University of Chinese Academy of Sciences, Beijing 100049, China*
[3]*School of Civil Engineering, Central South University, Changsha 410075, China*
[4]*National Engineering Laboratory for High Speed Railway Construction, Changsha 410075, China*

Correspondence should be addressed to Yulin Feng; fylin119@csu.edu.cn

Received 30 July 2019; Revised 8 September 2019; Accepted 19 September 2019; Published 16 October 2019

Academic Editor: Salvatore Grasso

To investigate the vibration analysis of elastically connected multiple beam system (ECMB) under the moving oscillator, finite sine-Fourier transform has been applied to the dynamic partial differential equations of ECMB with respect to space coordinates. Then, the numerical integration has been used to solve the equations. Finally, the expression for vibration analysis of ECMB under the moving oscillator has been derived based on finite sine-Fourier inverse transform. Using the method developed in this study and ANSYS numerical method, the vibration analysis of a four-layer beam system under moving oscillator with different speeds has been calculated. The results show that the calculated results from the method developed in this study are in good agreement with the ANSYS numerical calculation results, and the differences between the two calculation results are all less than 2%, which verified the correctness of the method developed in this study. The method developed in this study has been applied to the beam-rail system on a railway line in China. The effect of the train speed and interlayer stiffness on the vibration of beam-rail system has been investigated. The results show that the maximum dynamic deflection of the rail under the train load is always near the midspan, while the maximum dynamic deflections of the track plate, base plate, and bridge occur after the train travel through the midspan. The interlayer stiffness has a larger impact on the vibration of the rail and the track plate and little impact on the vibration of the base plate and the bridge.

1. Introduction

Beam-type structures are widely used in mechanical, civil, rail transportation, material engineering, and other fields. In engineering applications, it is of great importance to predict the dynamic response of beam-type structures accurately [1, 2].

Hitherto, there are many studies conducted by researchers all over the world on the dynamic response of beam-type structures under a moving oscillator. Also, there are many studies on the dynamic response of single-beam under a moving oscillator [3–5]. An important extension to the concept of single-beam is the double-beam system. The dynamic response of double-beam under a moving oscillator was investigated by different methods [6, 7]. Due to the complexity of the three-beam, the previous studies on the vibration problems of three-beam under a moving oscillator were mostly aimed at its vibration characteristics [8].

In many engineering applications, the vibration theory of single-beam, double-beam, and three-beam cannot meet the requirement. Therefore, it is urgently required to develop a method which can determine the vibration response of ECMB. Hitherto, there are only a few studies on the vibration problem of ECMB. Rao [9] investigated the natural vibrations of elastically connected multi-Timoshenko beams. Kelly and Srinivas [10] developed a general theory for the free response of elastically connected axially loaded beams. A set of coupled partial differential equations that govern the free response of a set of n elastically connected axially loaded beams has been developed and

nondimensionalized. Using Timoshenko and high-order shear deformation theory, Stojanović et al. [11] investigated a general procedure for the determination of the natural frequencies and buckling load for a set of beam system under compressive axial loading. Ariaei et al. [12] investigated the dynamic behavior of n parallel identical elastically connected Timoshenko beams subjected to a moving load. A relatively new computed approach called the Adomian modified decomposition method has been used to analyze the free vibration problem for an elastically connected multiple beam with arbitrary boundary conditions [13]. Through a differential transform method, a new procedure for determining natural frequencies and mode shapes of a system of elastically connected multiple rotating tapered beams has been presented [14]. Bakhshi Khaniki and Hosseini-Hashemi [15] investigated the dynamical behavior of ECMBs with respect to a moving mass. For double- and three-layered microbridge systems, using Laplace transform, an analytical solution has been developed. Moreover, for higher-layered microbridge systems, a state space method has been used. Hashemi and Bakhshi Khaniki [16, 17] studied the forced vibration of multilayered nanobeam systems (MLNBS) under a moving nanoparticle. Eringen's nonlocal theory and Euler Bernoulli beam theory were used to model each layer of the MLNBS. It was shown that nonlocality has a significant effect in analyzing such systems. Kargarnovin et al. [18] proposed a closed-form solution to study the dynamics of a composite beam with a single delamination under the action of a moving constant force; the delaminated beam was divided into four interconnected beams using the delamination limits as their boundaries. In summary, most of the current research methods for the vibration response of double-beam and three-beam systems under a moving oscillator have complicated derivation, with low computational efficiency and many limiting conditions. There are only a few studies on the vibration response of ECMBs.

In the present paper, based on the finite sine-Fourier transform, a method for calculating the vertical vibration response of ECMB under the moving oscillator has been developed. This method has the advantages of fewer constraints, higher computational efficiency, and a wider range of application. A comparison of the calculated results using this method, ANSYS numerical method, and existed literature showed that they are in good agreement. Therefore, the correctness of the method developed in this study has been verified. The problem of a dynamic response of beams subjected to moving oscillators is a reasonable idealization of how railway tracks and pavements behave under wheel load. This problem has been studied in some of above-mentioned studies [19–22]. Further, a beam-rail system on a railway line in China has been used as a case study. By simplifying the train into an oscillator system, the effect of the train speed on the dynamic deflection and amplification coefficient of beam-rail system and the effect of interlayer stiffness on the dynamic deflection of the midspan of beam-rail system have been analyzed.

The original contribution of this article is to consider an elastically connected multiple beam system subjected to a moving oscillator, and the semianalytical expression form of this article is easy to solve, which results in high computational efficiency. The semianalytical method can provide a theoretical basis for deriving a practical formula for engineering calculation and make up the deficiency of numerical simulation analysis. This study could be useful in different subjects of science, e.g., mechanical, civil, traffic, and material engineering and many other fields. For example, the dynamic behavior of the bridge-track system of railway (maglev) under the train load or multilayered nanobeam systems as a part of nanostructures has achieved more usages with improvements done in nanotechnology and the usage of smaller devices in designing different machines.

2. Mathematical Model and Governing Equations

2.1. Governing Equations of ECMB under the Moving Oscillator. The schematic diagram for ECMB under a moving oscillator is shown in Figure 1. All of beams are homogeneous and prismatic and have the same length L, but they can have different mass or flexural rigidities, which makes the model more real in reflecting some actual engineering projects. According to the d'Alembert principle, the dynamic equilibrium equation of an oscillator system is

$$M_2\frac{\partial^2 Z(t)}{\partial t^2} + k_0\left(Z(t) - y_1\right) = 0. \tag{1}$$

According to the d'Alembert principle, the dynamic equilibrium equations of ECMB are

$$E_1 I_1\frac{\partial^4 y_1}{\partial x^4} + m_1\frac{\partial^2 y_1}{\partial t^2} + k_1\left(y_1 - y_2\right) = P_0(t), \tag{2}$$

$$E_2 I_2\frac{\partial^4 y_2}{\partial x^4} + m_2\frac{\partial^2 y_2}{\partial t^2} - k_1\left(y_1 - y_2\right) + k_2\left(y_2 - y_3\right) = 0, \tag{3}$$

$$E_3 I_3\frac{\partial^4 y_3}{\partial x^4} + m_3\frac{\partial^2 y_3}{\partial t^2} - k_2\left(y_2 - y_3\right) + k_3\left(y_3 - y_4\right) = 0, \tag{4}$$

$$\cdots$$

$$E_{n-1} I_{n-1}\frac{\partial^4 y_{n-1}}{\partial x^4} + m_{n-1}\frac{\partial^2 y_{n-1}}{\partial t^2} - k_{n-2}\left(y_{n-2} - y_{n-1}\right) + k_{n-1}\left(y_{n-1} - y_n\right) = 0, \tag{5}$$

$$E_n I_n\frac{\partial^4 y_n}{\partial x^4} + m_n\frac{\partial^2 y_n}{\partial t^2} + k_{n-1}\left(y_n - y_{n-1}\right) = 0, \tag{6}$$

$$P_0(t) = \delta(x - vt)\left[(M_1 + M_2)g - M_1\left(\frac{\partial^2 y_1}{\partial t^2} + 2v\frac{\partial^2 y_1}{\partial x\,\partial t} + v^2\frac{\partial^2 y_1}{\partial x^2}\right) + k_0\left(Z(t) - y_1\right)\right], \tag{7}$$

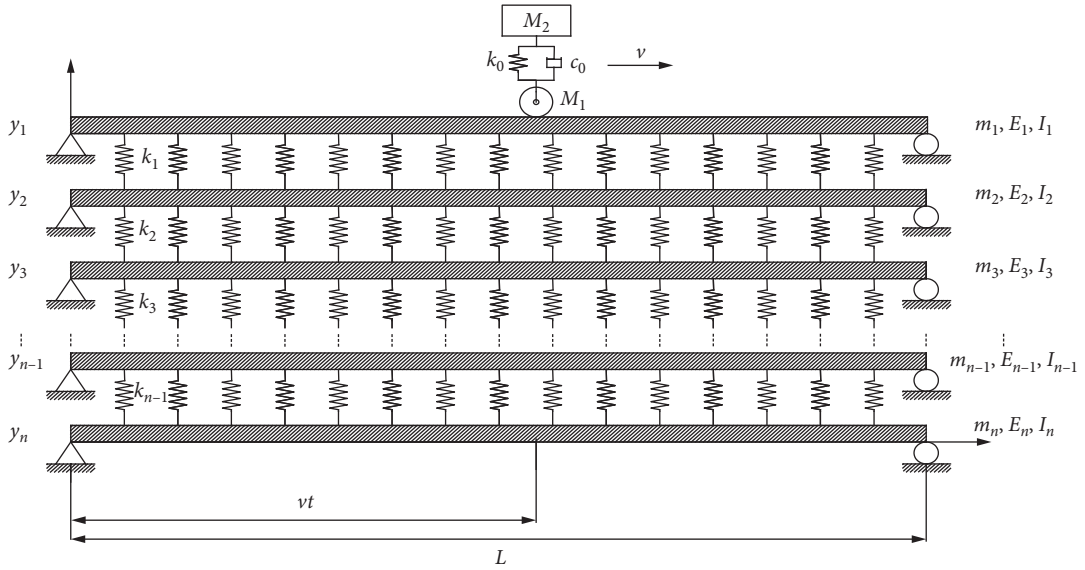

Figure 1: The schematic diagram for ECMB.

where $y_n(x,t)$, E_n, I_n, and m_n with $n = 2, 3, 4, \ldots$ are the dynamic deflection, elastic modulus, horizontal inertia moment, and beam mass per unit length for each layer of beam, respectively; M_1 and M_2 are the unsprung mass and sprung mass, respectively; and $Z(t)$ is the dynamic deflection of the sprung mass, and it is assumed that the unsprung mass moves along the beam without separating from the beam body. In this way, the deflection of unsprung mass is the same as that of the beam segment at the same location; k_0 and c_0 are the spring coefficient and damping coefficient of an oscillator system, respectively; k_{n-1} with $n = 2, 3, 4, \ldots$ is the interlayer spring stiffness; δ is Dirac function; v is the moving speed of the oscillator; $P_0(t)$ is the external force; and g is the gravitational acceleration.

2.2. Finite Sine-Fourier Transform. In order to solve equations (1)–(7), the finite sine-Fourier transform has been used and the transformation is defined as follows [23]:

$$\wp\left[y_n(x,t)\right] = U_{n,k}(t) = \int_0^L y_n(x,t)\sin\left(\xi_k x\right)\mathrm{d}x, \tag{8}$$

$$\wp^{-1}\left[U_{n,k}(t)\right] = y_n(x,t) = \frac{2}{L}\sum_{k=1}^{\infty} U_{n,k}(t)\sin\left(\xi_k x\right), \tag{9}$$

$$\xi_k = \frac{k\pi}{L}, \quad k = 1, 2, 3, \ldots. \tag{10}$$

For a small deformation, the boundary conditions of ECMB are

$$\begin{aligned} y_n(x,t)\big|_{x=0,L} &= 0, \\ EIy_n''(x,t)\big|_{x=0,L} &= 0. \end{aligned} \tag{11}$$

Based on the boundary conditions [24], the finite sine-Fourier transform of the fourth derivative of the displacement function with respect to the coordinate x is

$$\wp\left\{\frac{\mathrm{d}^4 y_n(x,t)}{\mathrm{d}x^2}\right\} = \xi_k^4 U_{n,k}(t). \tag{12}$$

Applying finite sine-Fourier transform with respect to the space coordinate x to both sides of equations (1)–(7) gives

$$\frac{L}{2}M_2\ddot{Z}(t) + \frac{L}{2}k_0 Z(t) - k_0\sum_{i=1}^{\infty} U_{1,i}(t)\sin\xi_i vt = 0, \tag{13}$$

$$\begin{aligned} &E_1 I_1 \xi_k^4 U_{1,k}(t) - M_1\frac{2}{L}v^2\sum_{i=1}^{\infty}\left(\xi_i\right)^2 U_{1,i}(t)\sin\xi_i vt\sin\xi_k vt \\ &\quad + k_0\frac{2}{L}\sum_{i=1}^{\infty} U_{1,i}(t)\sin\xi_i vt\sin\xi_k vt + m_1\ddot{\mathbf{U}}_{1,k}(t) \\ &\quad + M_1\sin\xi_k vt\frac{2}{L}\sum_{i=1}^{\infty}\ddot{\mathbf{U}}_{1,i}(t)\sin\xi_i vt + k_1 U_{1,k}(t) \\ &\quad - k_1 U_{2,k}(t) + M_1\frac{4}{L}v\sin\xi_k vt\sum_{i=1}^{\infty}\xi_i\dot{\mathbf{U}}_{1,i}(t)\cos\xi_i vt \\ &\quad - k_0\left(Z(t)\right)\sin\xi_k vt = \left(M_1 + M_2\right)g\sin\xi_k vt, \end{aligned} \tag{14}$$

$$\begin{aligned} &E_2 I_2 \xi_k^4 U_{2,k}(t) + m_2\frac{\partial^2}{\partial t^2}U_{2,k}(t) - k_1\left(U_{1,k}(t) - U_{2,k}(t)\right) \\ &\quad + k_2\left(U_{2,k}(t) - U_{3,k}(t)\right) = 0, \end{aligned} \tag{15}$$

$$\begin{aligned} &E_3 I_3 \xi_k^4 U_{3,k}(t) + m_3\frac{\partial^2}{\partial t^2}U_{3,k}(t) - k_2\left(U_{2,k}(t) - U_{3,k}(t)\right) \\ &\quad + k_3\left(U_{3,k}(t) - U_{4,k}(t)\right) = 0, \\ &\quad \ldots \end{aligned} \tag{16}$$

$$E_{n-1}I_{n-1}\xi_k^4 U_{n-1,k}(t) + m_{n-1}\frac{\partial^2}{\partial t^2}U_{n-1,k}(t) - k_{n-2}\left(U_{n-2,k}(t) - U_{n-1,k}(t)\right) + k_{n-1}\left(U_{n-1,k}(t) - U_{n,k}(t)\right) = 0, \tag{17}$$

$$E_n I_n \xi_k^4 U_{n,k}(t) + m_n\frac{\partial^2}{\partial t^2}U_{n,k}(t) + k_{n-2}\left(U_{n,k}(t) - U_{n-2,k}(t)\right) = 0. \tag{18}$$

Although k and i in the above equations are between $1 \sim \infty$, taking N items can generally meet the accuracy requirement.

Further, equations (13)–(18) can be expressed as

$$\mathbf{M}_{i,k}\ddot{\mathbf{U}}_k + \mathbf{C}_{i,k}\dot{\mathbf{U}}_k + \mathbf{K}_{i,k}\mathbf{U}_k = \mathbf{P}_k(t), \tag{19}$$

where

$$\mathbf{U}_k = \left[U_{1,k}\ U_{2,k}\ U_{3,k}\ \cdots\ U_{n-1,k}\ U_{n,k}\ Z\right]^T,$$
$$\mathbf{P}_k(t) = \left\{\mathbf{F}_1\ \mathbf{F}_2\ \mathbf{F}_3\ \cdots\ \mathbf{F}_{n-1}\ \mathbf{F}_n\ F_z\right\}^T,$$
$$\mathbf{M}_{i,k} = \mathrm{diag}\left[\mathbf{M}_{11}\ \mathbf{M}_{22}\ \mathbf{M}_{33}\ \cdots\ \mathbf{M}_{n-1n-1}\ \mathbf{M}_{nn}\ M_{zz}\right],$$
$$\mathbf{C}_{i,k} = \mathrm{diag}\left[\mathbf{C}_{11}\ \mathbf{0}_{i\times k}\ \mathbf{0}_{i\times k}\ \cdots\ \mathbf{0}_{i\times k}\ \mathbf{0}_{i\times k}\ \mathbf{0}\right],$$
$$\mathbf{K}_{i,k} = \begin{bmatrix} \mathbf{K}_{11} & -\mathbf{K}_{12} & \mathbf{0}_{i\times k} & \cdots & \mathbf{0}_{i\times k} & \mathbf{0}_{i\times k} & -\mathbf{K}_{1z} \\ & \mathbf{K}_{22} & -\mathbf{K}_{23} & \cdots & \mathbf{0}_{i\times k} & \mathbf{0}_{i\times k} & \mathbf{0}_{i\times 1} \\ & & \mathbf{K}_{33} & \cdots & \mathbf{0}_{i\times k} & \mathbf{0}_{i\times k} & \mathbf{0}_{i\times 1} \\ & & & \ddots & \vdots & \vdots & \vdots \\ & & & & \mathbf{K}_{n-1n-1} & -\mathbf{K}_{n-1n} & \mathbf{0}_{i\times 1} \\ & & & & & \mathbf{K}_{nn} & \mathbf{0}_{i\times 1} \\ \mathrm{syms} & & & & & & \mathbf{K}_{zz} \end{bmatrix}, \tag{20}$$

where $\mathbf{M}_{11}$, $\mathbf{M}_{22}$, $\mathbf{M}_{33}$, $\mathbf{M}_{n-1n-1}$, $\mathbf{M}_{nn}$, $\mathbf{C}_{11}$, $\mathbf{K}_{22}$, $\mathbf{K}_{33}$, K_{12}, $\mathbf{K}_{23}$, $\mathbf{K}_{21}$, $\mathbf{K}_{32}$, $\mathbf{K}_{n-1n-1}$, $\mathbf{K}_{nn}$, $\mathbf{K}_{n-1n}$, and $\mathbf{K}_{nn-1}$ are all $i \times k$ matrices and $\mathbf{K}_{1z}$ and $\mathbf{F}_1, \mathbf{F}_2, \mathbf{F}_3, \ldots, \mathbf{F}_{n-1}, \mathbf{F}_n$ are $i \times 1$ matrices.

2.3. Solution of Equations. As the position of the moving oscillator on ECMB changes with time, the mass matrix $\mathbf{M}_{i,k}$, the damping matrix $\mathbf{C}_{i,k}$ and the stiffness matrix $\mathbf{K}_{i,k}$ in equation (19) also all change with time t. Hence, the dynamic equilibrium equations for the coupling system of ECMB under moving oscillator are differential equations with time-varying coefficients. Further, the coefficient matrices $\mathbf{M}_{i,k}$, $\mathbf{C}_{i,k}$, and $\mathbf{K}_{i,k}$ also vary with the change in the speed v. The reaction of the entire structural system is calculated step by step at every time increment Δt, and the imbalance of the system within Δt is usually ignored in the calculation. On the other hand, the time-varying characteristic of the system is approximated by a series of constantly changing time-invariant systems. Therefore, the method of $Newmark - \beta$ is used in this study to solve equation (19).

$\mathbf{U}_k(t + \Delta t)$, $\dot{\mathbf{U}}_k(t + \Delta t)$, and $\ddot{\mathbf{U}}_k(t + \Delta t)$ are the displacement, velocity, and acceleration at time $t + \Delta t$, respectively, and they have been set to satisfy the dynamical equation (19) as follows:

$$\mathbf{M}_{i,k}\ddot{\mathbf{U}}_k(t + \Delta t) + \mathbf{C}_{i,k}\dot{\mathbf{U}}_k(t + \Delta t) + \mathbf{K}_{i,k}\mathbf{U}_k(t + \Delta t) = \mathbf{P}_k(t). \tag{21}$$

The displacement, velocity, and acceleration at the initial time are as follows:

$$\mathbf{U}_k(0) = 0, \quad \dot{\mathbf{U}}_k(0) = 0, \quad \ddot{\mathbf{U}}_k(0) = 0. \tag{22}$$

Using the $Newmark - \beta$ method, the velocity and displacement at time $t + \Delta t$ are

$$\dot{\mathbf{U}}_k(t + \Delta t) = \dot{\mathbf{U}}_k(t) + \left[(1 - \gamma)\ddot{\mathbf{U}}_k(t) + \gamma\ddot{\mathbf{U}}_k(t + \Delta t)\right]\Delta t,$$
$$\mathbf{U}_k(t + \Delta t) = \mathbf{U}_k(t) + \dot{\mathbf{U}}_k(t)\Delta t + \left[\left(\frac{1}{2} - \beta\right)\ddot{\mathbf{U}}_k(t) + \beta\ddot{\mathbf{U}}_k(t + \Delta t)\right]\Delta t^2, \tag{23}$$

where γ and β are the parameters of the $Newmark - \beta$ method.

Further, the acceleration, velocity, and displacement at time $(t + \Delta t)$ are

$$\ddot{\mathbf{U}}_k(t + \Delta t) = \frac{\mathbf{U}_k(t + \Delta t) - \mathbf{U}_k(t)}{\beta\Delta t^2} - \frac{\dot{\mathbf{U}}_k(t)}{\beta\Delta t} - \frac{\ddot{\mathbf{U}}_k(t)}{(2\beta) - 1},$$
$$\dot{\mathbf{U}}_k(t + \Delta t) = \dot{\mathbf{U}}_k(t) + \Delta t(1 - \gamma)\ddot{\mathbf{U}}_k(t) + \gamma\Delta t\ddot{\mathbf{U}}_k(t + \Delta t),$$
$$\mathbf{U}_k(t + \Delta t) = \left[\mathbf{K}_{i,k} + \frac{\mathbf{M}_{i,k}}{\beta\Delta t^2} + \frac{\mathbf{C}_{i,k}\gamma}{\beta\Delta t}\right]^{-1} \cdot \left[\mathbf{P}_k(t + \Delta t) + \mathbf{M}_{i,k}\left(\frac{\mathbf{U}_k(t)}{\beta\Delta t^2} + \frac{\dot{\mathbf{U}}_k(t)}{\beta\Delta t} + \frac{\ddot{\mathbf{U}}_k(t)}{(2\beta) - 1}\right) + \mathbf{C}_{i,k}\left(\frac{\mathbf{U}_k(t)\gamma}{\beta\Delta t} + \frac{\dot{\mathbf{U}}_k(t)}{\beta - 1} + \ddot{\mathbf{U}}_k(t)\left(\frac{\Delta t}{2}\right)\left(\frac{\gamma}{\beta} - 2\right)\right)\right]. \tag{24}$$

By substituting $\mathbf{U}_k$ into equation (9), we can obtain

$$\mathbf{y} = \frac{2}{L}\sum_{k=1}^{N}\mathbf{U}_k \sin\xi_k x, \tag{25}$$

where $\mathbf{y} = (y_1, y_2, y_3, \ldots, y_{n-1}, y_n)^T$.

3. Method Validation

To validate the accuracy of the method developed in this study for calculating the dynamic response of ECMB under a moving oscillator, a four-layer beam system is taken as an example. Using the MATLAB program and ANSYS numerical method, the vibration analysis of a four-layer beam system has been calculated for four moving speeds. Taking a four-story beam system as an example, using the MATLAB program and ANSYS numerical method, the vibration analysis of a four-layer beam system has been calculated for four moving speeds (i.e., 16 m/s, 32 m/s, 128 m/s, and 160 m/

s). Furthermore, the results of the dynamic response time-history curves and the peak of vibration analysis of the midspan deflection have been compared [25]. A comparison of results from the Matlab program and ANSYS numerical calculations is shown in Table 1 and Figure 2. In addition, the multilayer beam system was degraded to a double-layer beam to compare with the methods of the existed literature conveniently, and then the dynamic response of double-layer beam under the moving oscillator was calculated and compared with the results of Wu and Gao's method [6]. The dynamic response peaks of each layer at the positions of $x = 2.5$ m, 5.0 m, and 7.5 m were, respectively, extracted as shown in Table 2.

In Table 1, L_{Ia}, L_{IIa}, L_{IIIa}, and L_{IIIIa} are ANSYS calculation results of the peak of vibration analysis of the midspan deflections of the first layer, second layer, third layer, and fourth layer, respectively. L_{Im}, L_{IIm}, L_{IIIm}, and L_{IIIIm} are the Matlab calculation results of the peak of vibration analysis of the midspan deflections of the first layer, second layer, third layer, and fourth layer, respectively. E_I, E_{II}, E_{III}, and E_{IIII} are the calculation errors between the Matlab program and ANSYS calculation results of the peaks of vibration analysis of the midspan deflections of the first layer, second layer, third layer, and fourth layer, respectively. In Figure 2, u_I, u_{II}, u_{III}, and u_{IIII} are the midspan dynamic deflections of the first layer, second layer, third layer, and fourth layer, respectively.

From Table 1, it can be seen that E_I, E_{II}, E_{III}, and E_{IIII} of four moving speeds are less than 1.89%, 1.23%, 0.91%, and −0.48%, respectively. Since the differences are small, the correctness of the method developed in this study has been verified. From Figure 2, it can be seen for the dynamic time-history curves of the midspan deflections at the first layer, second layer, third layer, and fourth layer, the Matlab program results are in good agreement with the ANSYS numerical calculation results. From Table 2, it could be seen that the deviation of the calculation results of two methods at different positions ($x = 2.5$ m, 5.0 m, and 7.5 m) is less than 1.8%. Since the differences are small, the correctness of the method developed in this study has been verified again.

The advantages of the method developed in this study in terms of higher number of layers in this paper for specific performance are as follows: the system studied in this paper consists of n identical beams, in general, when much more layers are considered, the coupled partial equations are difficult to solve. Compared with the literature [12], this paper does not need to build a special relation of the stiffness of intermediate springs for decoupling the equation of motion; with the finite sine-Fourier transform, the equations can be uncoupled and solved. Compared with the literature [6], when studying the vibration of double-beam system, this paper does not need to divide into the vibration of two single-beam systems subjected to the same force, interlayer stiffness, damping, material properties of each layer, and moving oscillator [19]. When the number of layers increases, only the increased layer needs to be input into Formula (19) after the finite sine-Fourier transform; as long as the appropriate value of k is chosen, the vibration of elastically connected multiple beam system under the moving oscillator can be carried out, where, although k is between $1 \sim \infty$, taking $N \geq 30$ items can generally meet the accuracy requirement of engineering calculation [26].

Table 1: Comparison of the dynamic response peaks of the midspan deflections of the four-layer beam system.

Computed result	Speed (m/s)			
	16	32	128	160
L_{Ia} (mm)	−0.55500	−0.55500	−0.93800	−0.98700
L_{Im} (mm)	−0.55183	−0.54953	−0.92658	−1.00572
L_{IIa} (mm)	−0.12100	−0.11500	−0.21300	−0.20500
L_{IIm} (mm)	−0.12082	−0.11464	−0.21318	−0.20751
L_{IIIa} (mm)	−0.10200	−0.09300	−0.17100	−0.15800
L_{IIIm} (mm)	−0.10225	−0.09290	−0.17102	−0.15944
L_{IIIIa} (mm)	−0.09060	−0.09230	−0.15000	−0.15200
L_{IIIIm} (mm)	−0.09070	−0.09210	−0.14960	−0.14975
E_I (%)	−0.57	−0.98	−1.22	1.89
E_{II} (%)	−0.15	−0.32	0.09	1.23
E_{III} (%)	0.25	−0.11	0.01	0.91
E_{IIII} (%)	0.11	−0.22	−0.27	−1.48

4. Analysis of Examples

Since the method developed in this study has been verified (Section 3), it has been applied to a 32 m span beam-rail system (rail, track plate, base plate, and bridge) on a line in China [6, 27], as shown in Figure 3. The train model has been simplified into a system consisting of wheel, spring, damper, and sprung mass. The material properties and geometric parameters of the beam-rail system are shown in Table 3.

4.1. Effect of Train Speed on the Vibration of the Beam-Rail System. Figure 4 shows the variations of the dynamic deflections of rail, track plate, base plate, and bridge when the train moves across the bridge at the low speeds (i.e. 8 m/s and 32 m/s), medium-high speeds (64 m/s and 80 m/s), and high speeds (128 m/s and 160 m/s). In Figure 4, w is the dynamic deflection and L_p is the position of the train on the bridge. Figure 5 shows the comparison between the curves of the dynamic deflections of the rail, track plate, base plate, and bridge and the train position on the bridge with $v = 32$ m/s and $v = 160$ m/s.

From Figures 4 and 5, it can be seen that when the train speed increases from 8 m/s to 200 m/s, the peaks of the vibration analysis of the rail, track plate, base plate, and bridge deflection in the beam-rail system all increase initially and then subsequently decrease, which shows that for the beam-rail system, there is a critical train speed. The maximum dynamic deflection always occurs near the midspan of the rail, and the excitation effect of the train has a significant effect only on the first order frequency of the rail. Hence, the investigation on the maximum dynamic deflection of the rail can be done by analyzing the maximum dynamic deflection at midspan only. However, the shapes of dynamic deflection curves of the track plate, base plate, and bridge vary with the

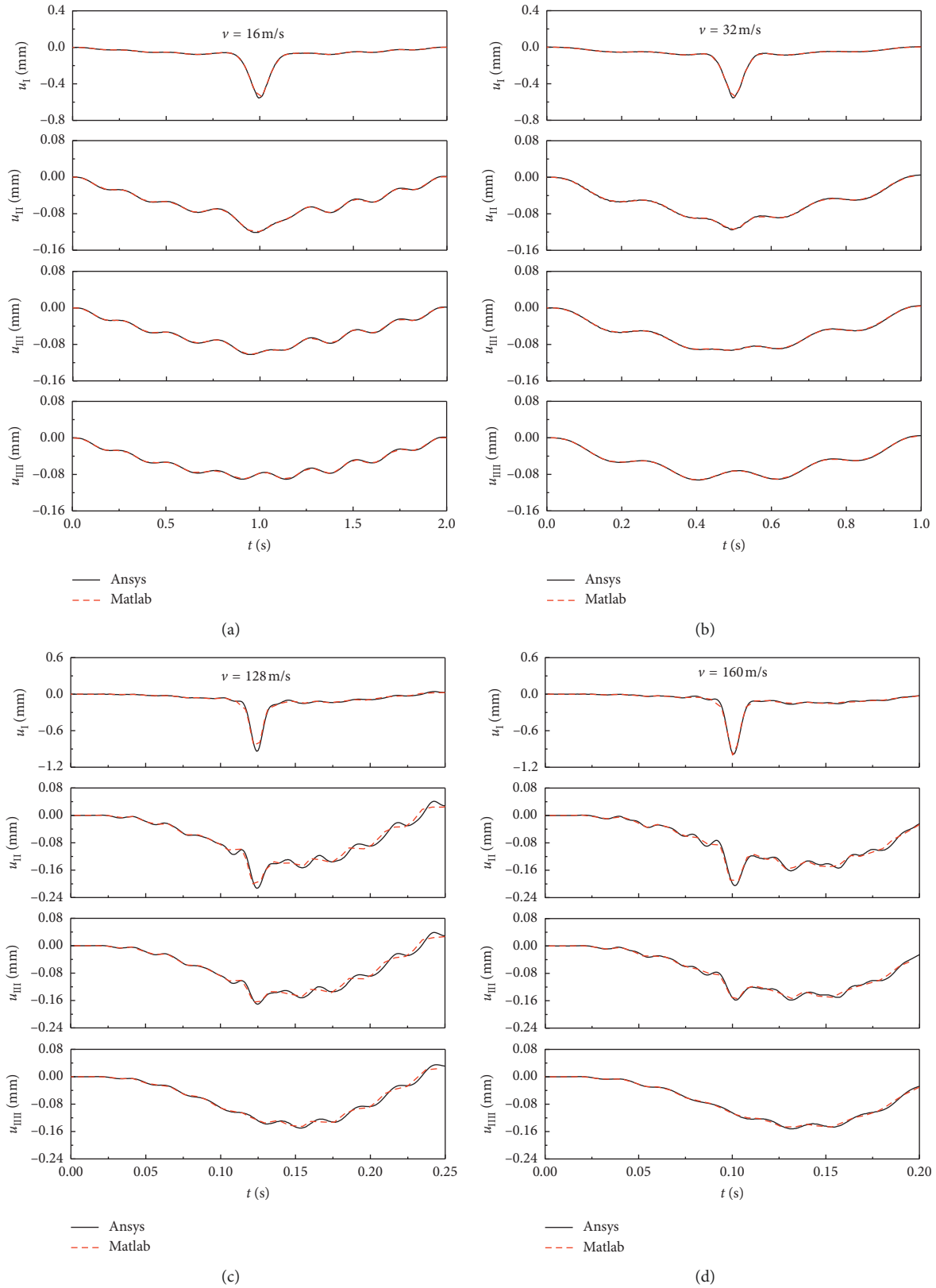

Figure 2: Comparison of dynamic response time-history curves of four-layer beam system under four moving speeds.

train speed, the dynamic response frequency increase with the train speed increase, and the position of the maximum dynamic deflection shifts from the midspan to the traveling direction of the train with the train speed increase. Further, it can be seen that the dynamic deflection response curves of the base plate and the bridge are basically the same. This is

Table 2: Comparison of dynamic response peaks at the positions of $x = 2.5$ m, 5.0 m, and 7.5 m.

Computed result	Calculation method	2.5	5.0	7.5
First layer	The proposed method/m	0.00753	0.01075	0.00743
	Wu and Gao's method [6]/m	0.00766	0.01083	0.00730
	Deviation	−1.69%	−0.74%	1.78%
Second layer	The proposed method/m	0.00481	0.006825	0.00484
	Wu and Gao's method [6]/m	0.00488	0.006820	0.00488
	Deviation	−1.43%	0.07%	−0.82%

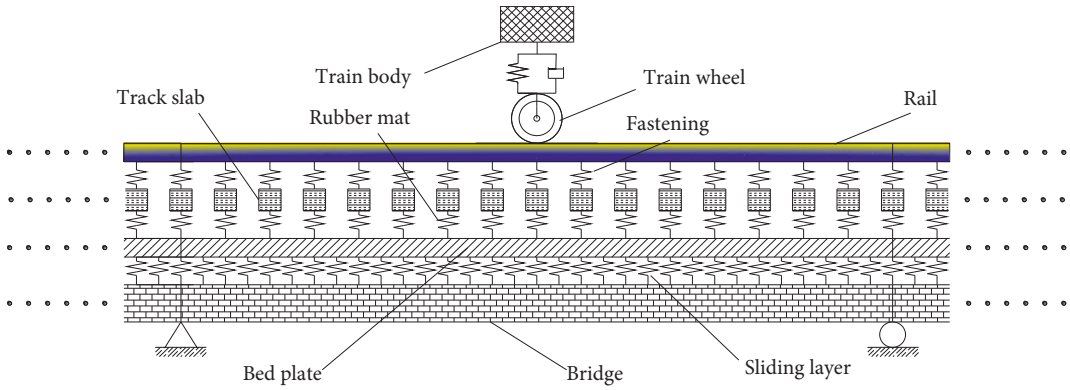

Figure 3: Simplified model of a railway line.

Table 3: Material properties and geometric parameters of the beam-rail system.

Parameter	Value
Rail	
Elastic modulus E_1	2.06×10^{11} N/m^2
Line mass m_1	60 kg/m
Moment of inertia I_1	3.217×10^{-5} m^4
Density ρ_1	7.85×10^3 kg/m^3
Track slab	
Line mass m_2	1275 kg/m
Density ρ_2	2.5×10^3 kg/m^3
Bed plate	
Elastic modulus E_3	3.00×10^{10} N/m^2
Line mass m_3	1401.25 kg/m
Moment of inertia I_3	1.6862×10^{-3} m^4
Density ρ_3	2.5×10^3 kg/m^3
Bridge	
Elastic modulus E_4	3.45×10^{10} N/m^2
Line mass m_4	36, 000kg/m
Moment of inertia I_4	10.42 m^4
Density ρ_4	2.5×10^3kg/m^3
Interlayer stiffness	
Stiffness of rail pad and fastener k_1	6×10^7 N/m^2
Stiffness of the sliding layer k_3	1.375×10^{12} N/m^2
Stiffness of the rubber pad under the supporting block k_2	9×10^8 N/m^2
Train	
Wheel mass M_1	2000 kg
Spring stiffness k_0	2.352×10^6 N/m
Car body mass M_2	11, 500 kg

due to the large vertical compressive stiffness of the sliding layer, which causes the base plate and the bridge to act as one unit.

4.2. Effect of Stiffness of Each Layer under the Rail on the Vibration of Beam-Rail System. For the train speed of 100 m/s, the effects of the fastener under the rail, the rubber pad under the supporting block, and the sliding layer stiffnesses on the vibration of the beam-rail system have been investigated. In each calculation, only one of three above stiffnesses has been changed, and the other two remain unchanged. Then, three different calculation schemes have been designed. For the stiffness of the fastener under the rail k_1 and the stiffness of the rubber pad under the supporting block k_2, the range is 40 MN/m^2~100 MN/m^2, with an increment of 10 MN/m^2. For the stiffness of the sliding layer k_3, the range is 500 MN/m^2~2e5 MN/m^2, with an increment of 100 MN/m^2. Figures 6–8 show the maximum dynamic deflections of the rail, track plate, base plate, and bridge corresponding to different stiffnesses of the fastener under the rail and the rubber pad under the supporting block and the sliding layer, respectively, where D_{peak} is the peak dynamic response of the midspan deflection.

From Figure 6, it can be seen that as the stiffness of the fastener under the rail increases, the maximum rail dynamic deflection decreases with a larger decrease in amplitude; the maximum dynamic deflection of the rail plate fluctuates at first and then gradually flattens, and the variations of the maximum dynamic deflections of the base plate and the

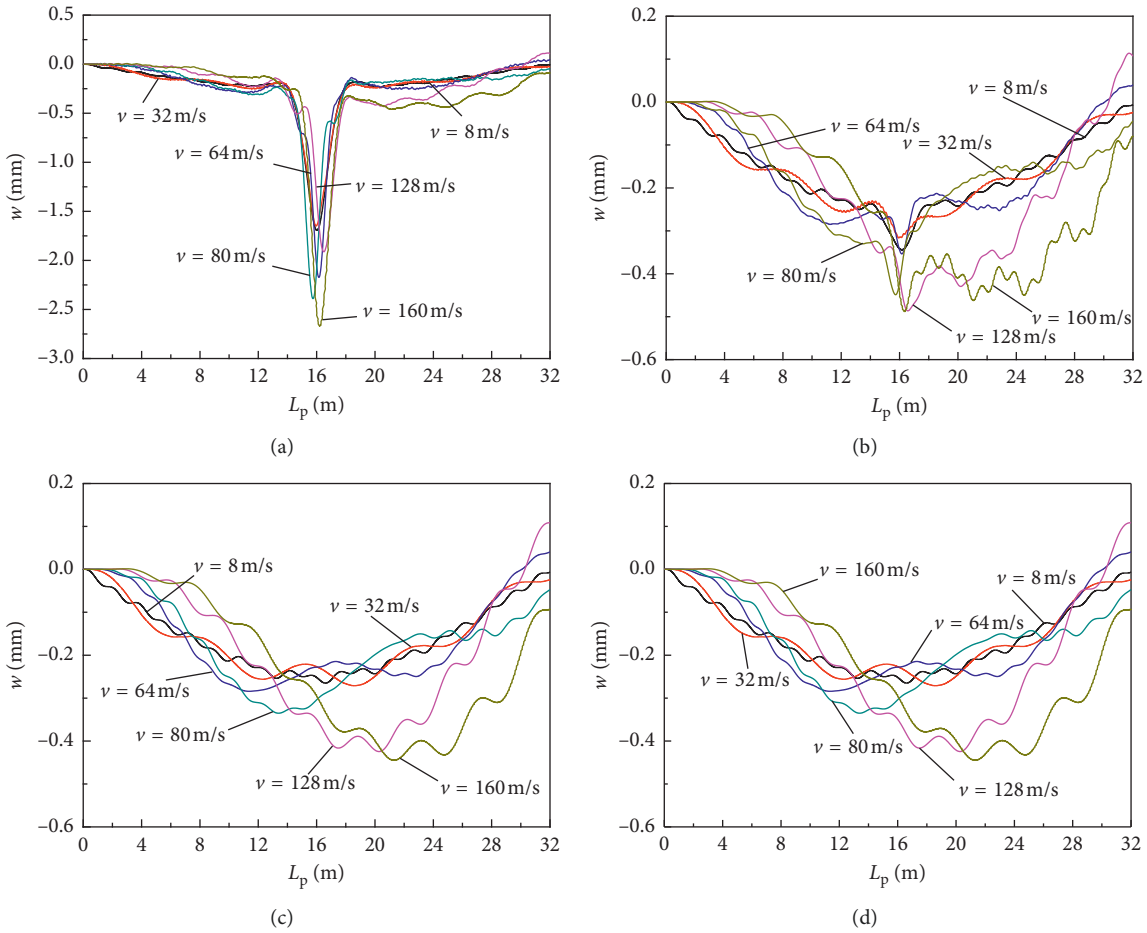

Figure 4: Dynamic deflections of rail, track plate, base plate, and bridge under different train speeds. Deflection of (a) rail, (b) track slab, (c) bed plate, and (d) bridge.

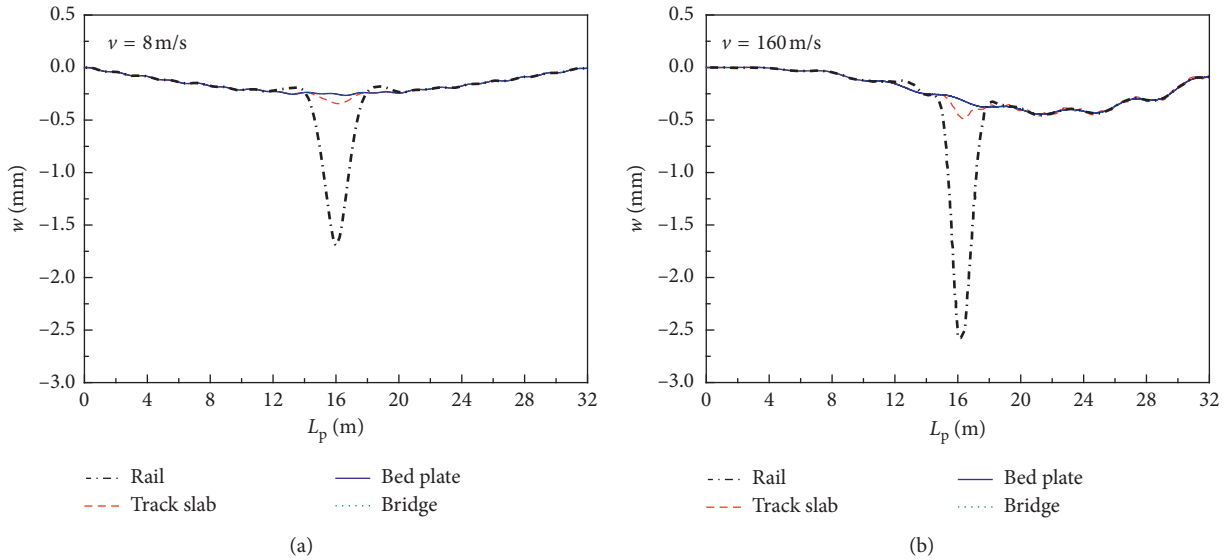

Figure 5: Comparison of dynamic deflection responses of rail, track plate, base plate, and bridge under different train speeds.

bridge are very small and they are basically the same. Therefore, the use of fasteners with high elasticity can effectively reduce the vibration of the rail. As shown in Figure 7, the stiffness of the rubber pad under the supporting block mainly affects the vibrations of the rail and the track plate. When the stiffness of the rubber pad increases from

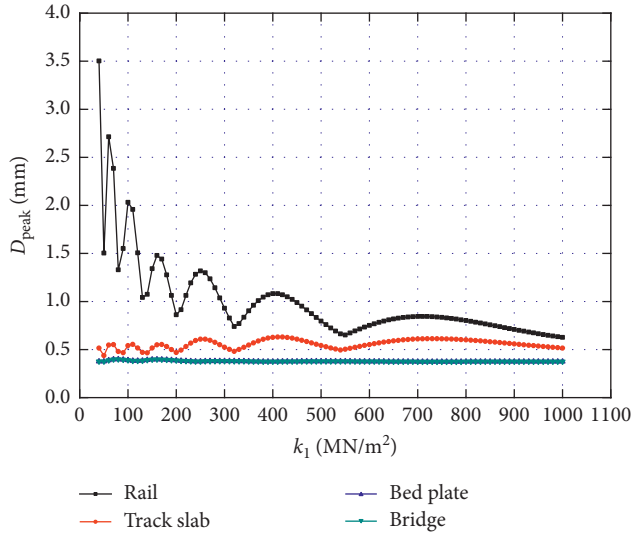

Figure 6: The maximum dynamic deflections of the rail, track plate, base plate, and bridge corresponding to different stiffnesses of the fastener under the rail.

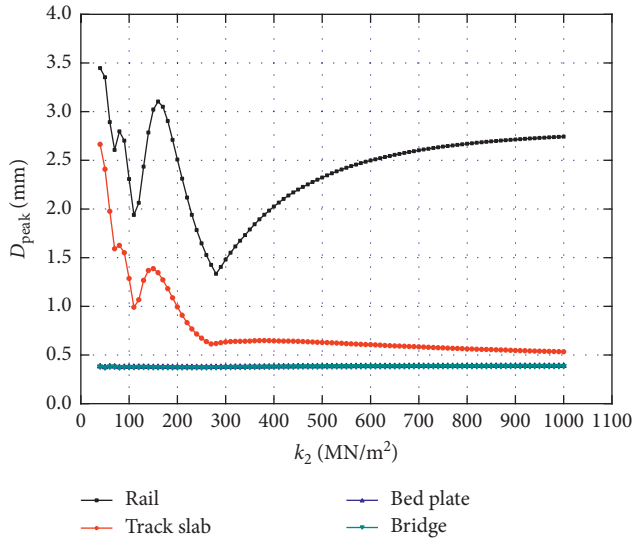

Figure 7: The maximum dynamic deflections of the rail, track plate, base plate, and bridge corresponding to different stiffnesses of the rubber pad under the supporting block.

40 MN/m^2 to 100 MN/m^2, the maximum dynamic deflection of the rail first fluctuates sharply and then flattens after reaching to a certain amplitude, the maximum dynamic deflection of the track plate also fluctuates drastically at first and then flattens after dropping to a certain value, and the maximum dynamic deflections of the base plate and the bridge remain practically unchanged. From Figure 8, it can be seen that as the stiffness of the sliding layer increases, the maximum rail dynamic deflection increases at first and then tends towards a constant value, the maximum dynamic deflection of the track plate and the base plate first decreases and then tends towards a constant value, and the maximum dynamic deflection of the bridge remains practically unchanged.

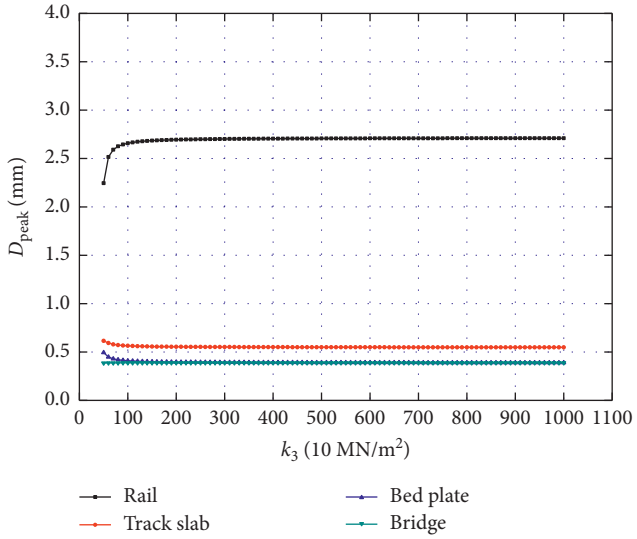

Figure 8: The maximum dynamic deflections of the rail, track plate, base plate, and bridge corresponding to different stiffnesses of the sliding layer.

5. Conclusions

Based on finite sine-Fourier inverse transform, the expression for dynamic response of a ECMB under a moving oscillator has been derived. Further, the vibration analysis of a four-layer simply supported beam system under moving oscillator with different speeds and the vibration analysis of a double-layer simply supported beam system under moving oscillator with different positions have been calculated. Comparing with the numerical methods developed in earlier studies, the method developed in this study has the advantages of clearer concept, simpler programming, and less computational effort. A beam-rail system on a line in China has been used as a case study, and the effect of the train speed and interlayer stiffness on the dynamic deflection and amplification coefficient of the midspan of the beam-rail system has been analyzed. Moreover, from the case study, the following conclusions have been obtained, which are meaningful to engineering design.

(1) The results show that the calculated results are in good agreement with those of ANSYS numerical and the existing literature. Hence, the correctness of the method developed in this study has been verified.

(2) This study could be useful in different subjects of science, e.g., mechanical, civil, traffic, and material engineering and many other fields. For example, the dynamic behavior of the bridge-track system of railway (maglev) under the train load or multi layered nanobeam systems as a part of nanostructures has achieved more usages with improvements done in nanotechnology and the usage of smaller devices in designing different machines.

(3) The vertical dynamic deflection of the rail in the beam-rail system under the train load always reaches a maximum near the midspan. The maximum

dynamic deflections of the track plate, base plate, and bridge may not occur when the train is located at the midspan but occurs after the train travels through the midspan.

(4) In the beam-rail system, there are several critical speeds which should be paid attention to and avoided in the practical engineering. The interlayer stiffness has a larger impact on the vibration of the rail and the track plate while it has a smaller impact on the vibration of the base plate and the bridge.

Data Availability

The data used to support the findings of this study are included within the article.

Conflicts of Interest

The authors declare that they have no conflicts of interest.

Acknowledgments

The research described in this paper was financially supported by the National Key Research and Development Program of China (No. 2017YFC0405101) and the National Natural Science Foundation of China (No. 91647103). The authors deeply thank Xilin Chai for his assistance in theoretical derivation and modification in this paper.

References

[1] Y. X. Li and L. Z. Sun, "Active vibration control of elastically connected double-beam systems," *Journal of Engineering Mechanics*, vol. 143, no. 9, Article ID 04017112, 2017.

[2] L. Jiang, Y. Feng, W. Zhou, and B. He, "Vibration characteristic analysis of high-speed railway simply supported beam bridge-track structure system," *Steel and Composite Structures*, vol. 31, no. 6, pp. 591–600, 2019.

[3] S. Eftekhar Azam, M. Mofid, and R. Afghani Khoraskani, "Dynamic response of timoshenko beam under moving mass," *Scientia Iranica*, vol. 20, no. 1, pp. 50–56, 2013.

[4] D. Mu and D.-H. Choi, "Dynamic responses of a continuous beam railway bridge under moving high speed train with random track irregularity," *International Journal of Steel Structures*, vol. 14, no. 4, pp. 797–810, 2014.

[5] C. P. S. Kumar, C. Sujatha, and S. Krishnapillai, "Non-uniform Euler-Bernoulli beams under a single moving oscillator: an approximate analytical solution in time domain," *Journal of Mechanical Science and Technology*, vol. 30, no. 10, pp. 4479–4487, 2016.

[6] Y. Wu and Y. Gao, "Dynamic response of a simply supported viscously damped double-beam system under the moving oscillator," *Journal of Sound and Vibration*, vol. 384, pp. 194–209, 2016.

[7] X. P. Wang and M. S. Li, "Analysis of vertical dynamic response of simply supported beam traversed by successive moving loads," *Applied Mechanics and Materials*, vol. 556–562, pp. 751–754, 2014.

[8] M. W. Hyer, W. J. Anderson, and R. A. Scott, "Non-linear vibrations of three-layer beams with viscoelastic cores, II: Experiment," *Journal of Sound and Vibration*, vol. 61, no. 1, pp. 25–30, 1978.

[9] S. S. Rao, "Natural vibrations of systems of elastically connected Timoshenko beams," *The Journal of the Acoustical Society of America*, vol. 55, no. 6, pp. 1232–1237, 1974.

[10] S. G. Kelly and S. Srinivas, "Free vibrations of elastically connected stretched beams," *Journal of Sound and Vibration*, vol. 326, no. 3–5, pp. 883–893, 2009.

[11] V. Stojanović, P. Kozić, and G. Janevski, "Exact closed-form solutions for the natural frequencies and stability of elastically connected multiple beam system using Timoshenko and high-order shear deformation theory," *Journal of Sound and Vibration*, vol. 332, no. 3, pp. 563–576, 2013.

[12] A. Ariaei, S. Ziaei-Rad, and M. Ghayour, "Transverse vibration of a multiple-Timoshenko beam system with intermediate elastic connections due to a moving load," *Archive of Applied Mechanics*, vol. 81, no. 3, pp. 263–281, 2011.

[13] Q. Mao, "Free vibration analysis of elastically connected multiple-beams by using the Adomian modified decomposition method," *Journal of Sound and Vibration*, vol. 331, no. 11, pp. 2532–2542, 2012.

[14] M. Ghafarian and A. Ariaei, "Free vibration analysis of a system of elastically interconnected rotating tapered Timoshenko beams using differential transform method," *International Journal of Mechanical Sciences*, vol. 107, pp. 93–109, 2016.

[15] H. Bakhshi Khaniki and S. Hosseini-Hashemi, "The size-dependent analysis of multilayered microbridge systems under a moving load/mass based on the modified couple stress theory," *The European Physical Journal Plus*, vol. 132, no. 5, p. 200, 2017.

[16] S. Hosseini Hashemi and H. Bakhshi Khaniki, "Dynamic behavior of multi-layered viscoelastic nanobeam system embedded in a viscoelastic medium with a moving nanoparticle," *Journal of Mechanics*, vol. 33, no. 5, pp. 559–575, 2017.

[17] S. H. Hashemi and H. B. Khaniki, "Dynamic response of multiple nanobeam system under a moving nanoparticle," *Alexandria Engineering Journal*, vol. 57, no. 1, pp. 343–356, 2018.

[18] M. H. Kargarnovin, M. T. Ahmadian, and R.-A. Jafari-Talookolaei, "Analytical solution for the dynamic analysis of a delaminated composite beam traversed by a moving constant force," *Journal of Vibration and Control*, vol. 19, no. 10, pp. 1524–1537, 2013.

[19] Y. Wu and Y. Gao, "Analytical solutions for simply supported viscously damped double-beam system under moving harmonic loads," *Journal of Engineering Mechanics*, vol. 141, no. 7, Article ID 04015004, 2015.

[20] G. Muscolino and A. Palmeri, "Response of beams resting on viscoelastically damped foundation to moving oscillators," *International Journal of Solids and Structures*, vol. 44, no. 5, pp. 1317–1336, 2007.

[21] B. Biondi, G. Muscolino, and A. Sofi, *A Substructure Approach for the Dynamic Analysis of Train-Track-Bridge System*, Pergamon Press, Oxford, UK, 2005.

[22] G. Muscolino, A. Palmeri, and A. Sofi, "Absolute versus relative formulations of the moving oscillator problem," *International Journal of Solids and Structures*, vol. 46, no. 5, pp. 1085–1094, 2009.

[23] W. Guo, Z. Zhai, Z. Yu, F. Chen, Y. Gong, and T. Tan, "Experimental and numerical analysis of the bolt connections in a low-rise precast wall panel structure system," *Advances in Civil Engineering*, vol. 2019, Article ID 7594132, 22 pages, 2019.

[24] Y. Zheng, H. Zhong, Y. Fang, W. Zhang, K. Liu, and J. Fang, "Rockburst prediction model based on entropy weight

integrated with grey relational BP neural network," *Advances in Civil Engineering*, vol. 2019, Article ID 3453614, 8 pages, 2019.

[25] Z. Huang, L. Z. Jiang, Y. F. Chen, Y. Luo, and W. B. Zhou, "Experimental study on the seismic performance of concrete filled steel tubular laced columns," *Steel and Composite Structures*, vol. 26, no. 6, pp. 719–731, 2019.

[26] Z. Ba, Z. Kang, and J. Liang, "In-plane dynamic Green's functions for inclined and uniformly distributed loads in a multi-layered transversely isotropic half-space," *Earthquake Engineering and Engineering Vibration*, vol. 17, no. 2, pp. 293–309, 2018.

[27] H. Gou, W. Zhou, Y. Bao, X. Li, and Q. Pu, "Experimental study on dynamic effects of a long-span railway continuous beam bridge," *Applied Sciences*, vol. 8, no. 5, p. 669, 2018.